

# Fracture Toughness of Si<sub>3</sub>N<sub>4</sub> Processed by Gas Pressure Sintering and Hot Pressing

Cláudio V. Rocha\*, Célio A. Costa\*

Programa de Engenharia Metalúrgica e de Materiais – PEMM/COPPE,  
Universidade Federal do Rio de Janeiro, Centro de Tecnologia, Bloco F,  
Sala 210, 21949-900 Rio de Janeiro - RJ, Brazil

Received: September 29, 2004; Revised: January 19, 2006

This present work evaluates the influence of microstructure on the fracture toughness of two types of silicon nitride. The two microstructural types of silicon nitride were processed using the gas pressure sintering (GPS) and hot pressing (HP) pathways. The fracture toughness was measured using the Single Edge V-Notch Beam (SEVNB) and Chevron Notch Beam (CNB) methods. The results from both methods for the two forms were in close agreement (with a maximum variation of 5.8%); the  $K_{Ic}$  of the material processed by HP was 35% higher than that of GPS and the grain length had a direct influence on the fracture toughness.

**Keywords:** fracture toughness, silicon nitride, gas pressure sintering, hot pressing

## 1. Introduction

Silicon nitride (Si<sub>3</sub>N<sub>4</sub>) is an advanced ceramic used in a variety of applications since it possesses high fracture toughness and strength, thermal shock resistance and good creep behavior. All these properties are related to the microstructure of the material, which depends on the manufacturing process and the method of test employed<sup>1</sup>.

A complete investigation of the fracture toughness properties is still under investigation due to the complexity of the technique itself and the microstructure present. For instance, pressureless sintered (PS) and gas pressure sintered (GPS) silicon nitride present rod-shaped grains that are randomly oriented, resulting in an isotropic microstructure<sup>2</sup>. On the other hand, hot-pressed (HP) Si<sub>3</sub>N<sub>4</sub> exhibits a certain amount of grain texture, since the elongated β-grains tend to be perpendicular to the hot-pressing direction<sup>3</sup>. These orientated grains are responsible for anisotropy of up to 20%<sup>1</sup> verified in the fracture toughness, strength and thermal conductivity<sup>4</sup> tests.

Accurate measurements of fracture toughness ( $K_{Ic}$ ) is relatively difficult for most ceramic materials. The major problems are: introduction of a sharp-notch, reproducibility, validity of equations, elimination of residual stresses and control of crack propagation. As a consequence, values of fracture toughness present little reproducibility and high dispersion, even when using the same techniques. Furthermore, if the material has a rising R-curve, each method tends to show different results. A unique, unambiguous, universally acceptable method to evaluate fracture toughness of structural ceramics is yet to emerge<sup>5</sup>.

The main object of this study is to correlate microstructure and fracture toughness. To fulfill this goal, two silicon nitride materials with distinct compositions were sintered by different routes, one by GPS and the other HP, and both were evaluated by two fracture toughness techniques, namely, Single Edge V-Notch Beam (SEVNB) and Chevron Notch Beam (CNB).

## 2. Experimental Procedures

The Si<sub>3</sub>N<sub>4</sub> materials (HP and GPS) were prepared using colloidal processing: ball milling with Si<sub>3</sub>N<sub>4</sub> balls in alcohol for 12 hours, drying and sieving. The GPS material, composed of α-Si<sub>3</sub>N<sub>4</sub>, 5% Y<sub>2</sub>O<sub>3</sub> and 3.5% Al<sub>2</sub>O<sub>3</sub>, was sintered at 1850 °C for 30 minutes with a N<sub>2</sub> pressure of 10 MPa. The HP material, on the other hand, was

composed of α-Si<sub>3</sub>N<sub>4</sub>, 10% β-Si<sub>3</sub>N<sub>4</sub> whiskers and 3% MgO, and was hot pressed at 1750 °C for 2 hours under a 32 MPa of uniaxial compressive stress (Nitrogen atmosphere). The whiskers presented an initial average length of 5.16 μm and width of 0.51 μm, resulting in an aspect ratio of 10.88.

The fracture toughness values were obtained by the SEVNB and CNB methods, with the specimen dimensions of 3 mm x 4 mm x 50 mm (W x D x L) for both of them, following ASTM C-1421. The SEVNB specimen was prepared in two steps: the opening of a straight notch with a diamond blade (0.15 mm thick) at the middle of the specimen on the 3 mm width surface. The notch depth was about 0.5 mm. The second step increased the depth of the opened notch slightly by polishing it with a razor blade sprinkled with diamond paste (1 μm). This procedure resulted in very sharp V<sup>6,7</sup> shape (Figure 1) where the notch-root radius has the same effect of a sharp crack and therefore allows a reliable determination of  $K_{Ic}$ . The introduction of a sharp notch was carried out on a plane jig supported by springs, as shown in Figure 2. The fixture assembly required rigidity, in such a way that the blade could not twist or bend over the specimens, but remained steady during the reciprocating movement of the machine. The use of the springs in the assembly allowed adjustment of the normal applied force on the specimens, since the table of the equipment controls the depth of the razor blade. The chevron notch (CNB method) was opened using a diamond cutter with a width of 0.15 mm, according to ASTM Standard C-1421<sup>8</sup>. An illustration of the CNB specimen can be seen in Figure 3.

The specimens were tested in four-point bending at a speed of 0.05 mm/min and the deflection of the specimens was measured by an LVDT. For the SEVNB method, the crack extended unstably when the external load reached a maximum value; whereas for the CNB, a stable crack propagation was induced. Both are mandatory requirements for the validation of the tests.

The expressions used to calculate the fracture toughness for CNB<sup>8</sup> and SEVNB<sup>9</sup> methods are presented in Equations 1 and 3, respectively:

$$K_{Ic} = Y *_{min} \left[ \frac{P_{max}(L - L_d) 10^{-6}}{B.W^{3/2}} \right] \quad (1)$$

\*e-mail: claudiov@metalmat.ufrj.edu.br, celio@metalmat.ufrj.edu.br

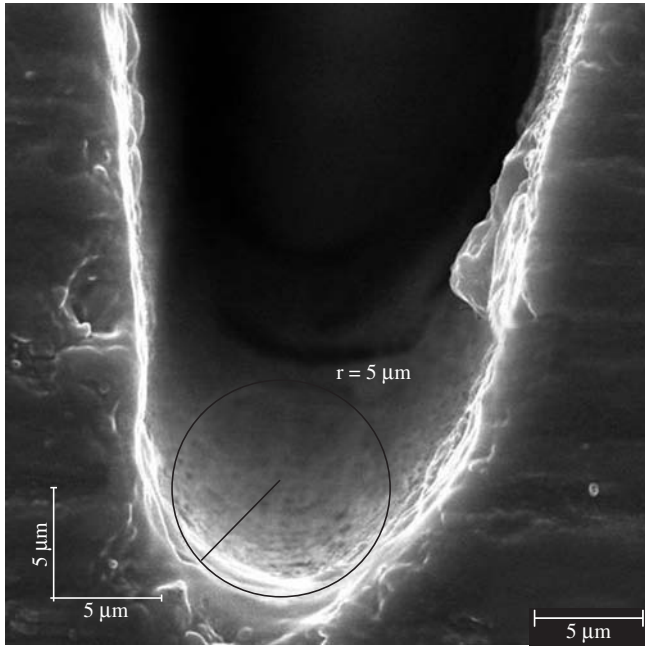


Figure 1. Micrograph of a V-notch: notch-root radius.

$$Y_{min}^* = \frac{0,5256 - 3,4872 (a_0/W) + 3,9861 (a_0/W) - 2,0038 (a_0/W)^2 + 0,5489 (a_0/W)^3}{1 - 2,9050 (a_0/W) + 2,7174 (a_0/W)^2 - 0,8963 (a_0/W)^3 + 0,0361 (a_0/W)^4} \quad (2)$$

$$K_{Ic} = \sigma \cdot \sqrt{a} \cdot Y = \frac{P_{max}}{B \cdot W^{1.5}} (L - L_0) \frac{3 \sqrt{\alpha}}{2(1 - \alpha)^{1.5}} \cdot Y' \quad (3)$$

$$Y' = 1,9887 - 1,326\alpha - (3,49 - 0,68\alpha + 1,35\alpha^2)\alpha(1 - \alpha)(1 + \alpha)^{-2} \quad (4)$$

With:  $\alpha = a/W$

Where:

$P_{max}$ : Maximum load (N);

$\sigma$ : Fracture stress (four-point bending) (Pa);

L: Outer (support) span (m);

$L_0$ : Inner (loading) span (m);

B: Dimension of the specimen perpendicular to the crack length (m);

W: Dimension of the specimen parallel to the crack length (m);

a: Notch depth (m);

$Y'$ : Stress intensity shape factor (dimension-less); and

$Y_{min}^*$ : Minimum stress intensity factor coefficient (dimension-less).

The rigidity of the test fixture is a very important parameter, especially for the CNB method, since a stable fracture must be observed for the test to be validated. To observe and quantify the grain structure, the surfaces were polished, etched with HF at 112 °C, observed in a SEM and digitally analyzed.

### 3. Results and Discussion

The good mechanical properties of  $Si_3N_4$  are attributed to the  $\alpha \rightarrow \beta$  phase transformation during the sintering process. This transformation changes the equiaxed  $\alpha$  into an idiomorphic  $\beta$  rod-like grain, which is directly responsible for the high fracture toughness behavior observed in this kind of material<sup>10</sup>. The sintering routes used here resulted in 99% dense materials (Table 1), measured using the Archimedes method, and in a complete  $\alpha \rightarrow \beta$  phase transformation.

The microstructures of the samples sintered by GPS and HP are shown in Figures 4 and 5, respectively. In both microstructures, the formation of elongated grains in a fine matrix, characteristic of the rod-like  $\beta-Si_3N_4$ <sup>11</sup> can be observed. However, in the material processed by GPS the elongated grains are a result of the  $\alpha \rightarrow \beta$  transformation, which is carried out in the presence of the liquid phase while in the hot-pressed material the elongated grains are mainly whiskers, which were added intentionally to increase fracture toughness. In both cases, the elongated  $\beta-Si_3N_4$  crystals provided higher resistance to crack growth since they are responsible for the toughening mechanisms present, for instance: crack bridging, crack deflection and grains/whiskers pull-out<sup>12</sup>. Nevertheless, there are some indications that other parameters such as the amount and properties of the glassy phase can also influence the mechanical properties both at room and high temperatures<sup>1</sup>. As a consequence, the stereological characterization becomes essential to correlate microstructure and properties; furthermore, as the microstructures are similar the use of SEM and digital image analysis were required for characterization.

As shown in Table 1, the HP material possessed an average grain length higher than GPS, which can be attributed to the whiskers added (10 wt. (%)) to the composition, even though the aspect ratio was almost reduced fourfold in the ball milling process. The presence of whiskers can form a three-dimensional network, which inhibits densification and hinders the growth of the transformed grains, which becomes equiaxed instead of rod-like, a behavior also mentioned by Costa and Todd<sup>13</sup>. On the other hand, the elongated grains of the

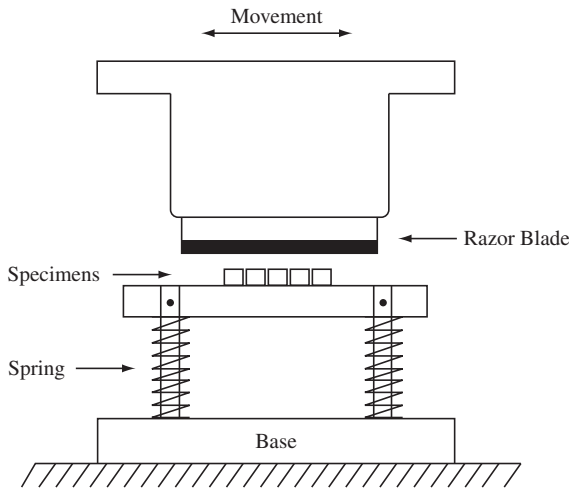


Figure 2. Assembly for the introduction of a sharp notch by the razor blade polishing technique.

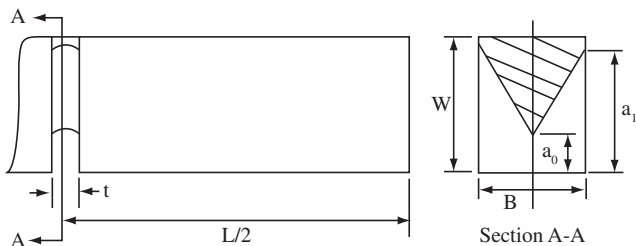
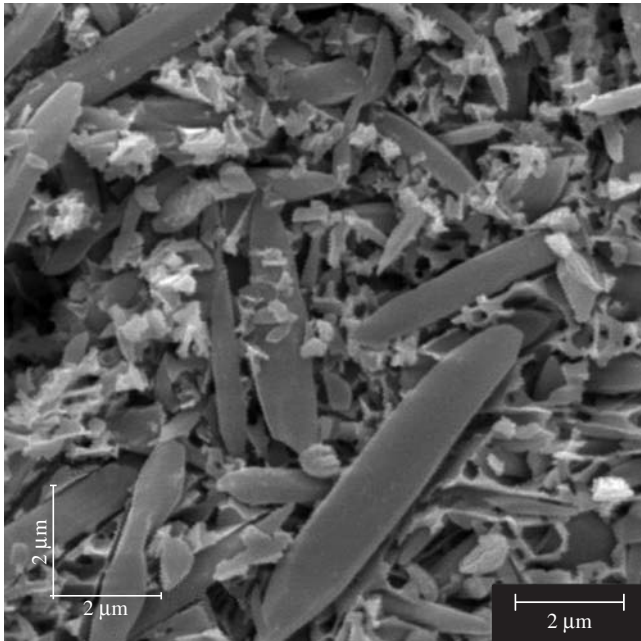
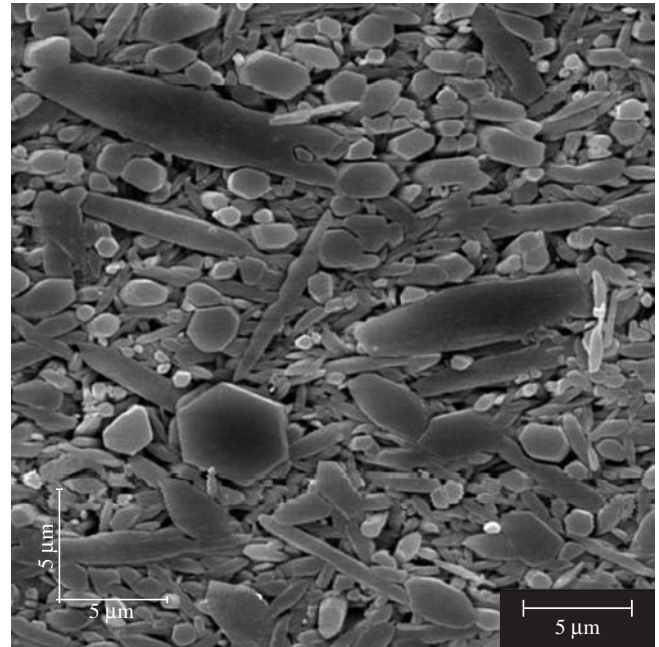


Figure 3. Chevron notch flexure specimen.

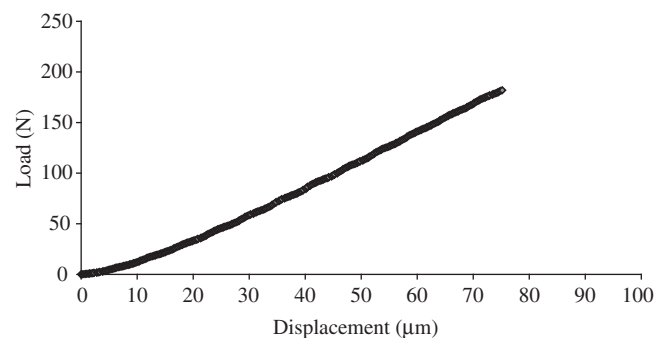
**Table 1.** Microstructural features and fracture toughness of the analyzed samples.

Sample	Microstructural features ( $\mu\text{m}$ )			Relative Density (%)	Fracture toughness ( $\text{MPa}\cdot\text{m}^{1/2}$ )			
	Length	Width	Aspect ratio		SEVNB	SD	CNB	SD
GPS	1.08	0.52	2.14	99.8	6.51	0.18	6.74	0.30
HP	1.32	0.52	2.67	99.1	8.81	0.08	9.32	0.23
(HP/GPS)	22.2%	0%	24.7%	-	35.3%	-	38.3%	-

**Figure 4.** Microstructure of GPS -  $\text{Si}_3\text{N}_4$ .**Figure 5.** Microstructure of HP -  $\text{Si}_3\text{N}_4$ .

GPS material were a result of the  $\alpha \rightarrow \beta$  transformation and their growth plays a reinforcement role, similar to the whiskers in the HP material. The grain width in both materials is equal as shown in (Table 1). This is independent of the sintering additive, processing routes, temperature and shelf time. This behavior suggests that either there is a saturation limit for this parameter or the combinations of time and temperature were equivalent. However these hypothesis need to be confirmed.

The fracture toughness results are also presented in the Table 1, and they represent the average of 5 valid tests, as recommended by ASTM C-1421. The  $K_{Ic}$  of the GPS material measured by the CNB method was 3.5% higher than that measured by SEVNB, and for the HP material, the CNB value obtained was 5.8% higher than the SEVNB method. Four possible explanations have been presented when  $K_{Ic}$  measured by different methods is not the same, either individually or in conjunction. Firstly, Quinn<sup>14</sup> noted that if stable crack extension occurs during the SEVNB tests an erroneous result will be obtained if the extension is not included in the calculation. However, in this work, the force-displacement curves for all valid tests did not shown the existence of stable crack extension during SEVNB tests, as shown in Figure 6, and so this explanation was disregarded. Secondly, an underestimation of the notch introduced into the specimens may result in higher fracture toughness value<sup>5</sup>, but the notch-root radius ( $\rho$ ) measured in the SEVNB specimens were very sharp, about  $5 \mu\text{m}$ , a value that is considered to make SEVNB- $K_{Ic}$  independent of the notch width<sup>7</sup>. Thirdly, the presence of residual stress<sup>5</sup>, which was considered to be null since the notches were opened carefully and

**Figure 6.** Load vs. Displacement profiles for the SEVNB method: catastrophic crack propagation.

any contribution was considered to be minor and not able to make significant changes in the results. And finally the existence of a rising R-curve behavior<sup>8</sup>. Even though the fracture toughness tests have not been performed with different crack lengths, the differences attained (3.5% and 5.8%) are very small and in the range reported in the literature for hot pressed silicon nitride<sup>8</sup>, about 4.5% measured by CNB, pre-cracked beam and surface crack in flexure. Regarding the CNB tests, the smooth nonlinear transition through to the maximum load, prior to the final fracture, indicative of stable crack extension, was obtained, as shown in Figure 7.

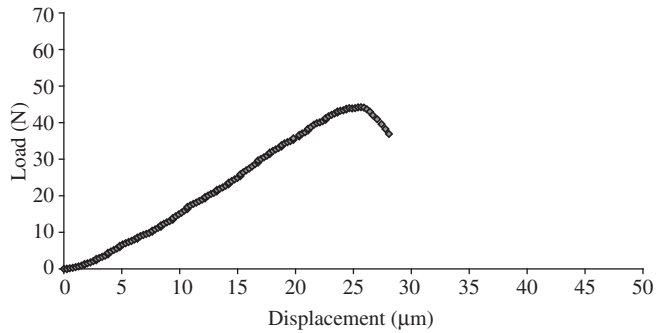


**Figure 7.** Load vs. Displacement profiles for the CNB method: stable crack propagation.

The microstructure of silicon nitride has a direct influence on toughening mechanisms, which affects the fracture toughness. Among the microstructural features, the grain length and the aspect ratio are the most important<sup>15</sup>, since there is a direct correlation between the microstructural features and the corresponding mechanical properties. The HP samples presented an average grain length and aspect ratio 22.2% and 24.7%, respectively, higher than the GPS samples. In the same way, the fracture toughness of the HP material measured by SEVNB and CNB was 35.3% and 38.3% higher, respectively, than observed for GPS. These results show that for the same grain width (0.52 mm) an increase in the grain length causes an immediate increase in the fracture toughness of silicon nitride, independent of the test method used. The direct influence of grain length on the increased fracture toughness was also observed by Tani's<sup>16</sup> and Peillon's<sup>17</sup> work, which optimized the amount of additive, sintering time and temperature of silicon nitride densified by GPS in order to obtain grain sizes of increased length. The effect of grain length may be a major player on  $K_{Ic}$ ; however, a few other features may also be responsible, for instance, the volumetric fraction of elongated grain preferentially aligned with the crack propagation path and the possible R-curve behavior in the HP material, an anisotropic material, particularly with respect to fracture toughness. So, it may be said that the grain length strongly influence  $K_{Ic}$  values, but other microstructural parameters cannot be disregarded.

Finally, the SEVNB and CNB methods can be considered accurate and reproducible to evaluate silicon nitride materials and other high density ceramics, since both methods showed a small scatter of the results (small standard deviation). Decision on which method to use should be based on the technical difficulties involved, principally, the introduction of sharp notches required to perform each technique.

#### 4. Conclusions

The samples of  $Si_3N_4$  processed by HP and GPS presented high  $K_{Ic}$  values, which were attributed to the addition of whiskers and "in situ" reinforcement, respectively. The  $K_{Ic}$  values for HP sample were higher than the GPS sample due, possibly, to addition of whiskers (10 wt. (%)) and their alignment perpendicularly to the hot pressing direction. The microstructure had a strong influence on the fracture toughness, where the HP samples presented higher grain length and aspect ratio than the GPS samples, resulting in higher values of  $K_{Ic}$ .

The results obtained by SEVNB and CNB showed that the maximum variation in  $K_{Ic}$  was 5.8%, a close agreement between the methods.

#### Acknowledgments

The authors would like to thank CNPq and FAPERJ for supporting this work.

#### References

- Ziegler G, Heinrich J, Wötting G. Review - Relationships between processing, microstructure and properties of dense and reaction-bonded silicon nitride. *Journal of Materials Science*. 1987; 22:3041-3086.
- Kondo N, Ohji T, Wakai F. Strengthening and toughening of silicon nitride by superplastic deformation. *Journal of the American Ceramic Society*. 1998; 81(3):713-716.
- Park D, Kim C. Anisotropy of silicon nitride with aligned silicon nitride whiskers. *Journal of the American Ceramic Society*. 1999; 82(3):780-782.
- Watairi K, Hirao K, Toriyama M, Ishizaki K. Effect of grain size on the thermal conductivity of  $Si_3N_4$ . *Journal of the American Ceramic Society*. 1999; 82(3):777-779.
- Mukhopadhyay A, Datta S, Chakraborty D. Fracture toughness of structural ceramics. *Ceramics International*. 1999; 25:447-454.
- Rausch G, Kuntz M, Grathwohl G. Determination of the in situ fiber strength in ceramic-matrix composites from crack-resistance evaluation using single-edge notched-beam test. *Journal of the American Ceramic Society*. 2000; 83(11):2762-2768.
- Damani R, Schuster C, Danzer R. Polished notch modification of SENB-S fracture toughness testing. *Journal of the European Ceramic Society*. 1997; 17:1685-1689.
- Standard test methods for determination of fracture toughness of advanced ceramics at ambient temperature. *ASTM - Designation: C-1421*. West Conshohocken, PA, USA: ASTM International; 1999.
- Kübler J. Fracture toughness of ceramics using the SEVNB method: from a preliminary study to a test method. In: Salem J, Quinn G, Jenkins, editors. *Fracture Resistance Testing of Monolithic and Composite Brittle Materials, ASTM STP 1409*. West Conshohocken, PA, USA: ASTM International; 2002. p. 93-106.
- Bowen L, Carruthers T. Development of mechanical strength in hot-pressed silicon nitride. *Journal of Materials Science Letters*. 1978; 13:684-687.
- Park D, Kim C. Indentation crack length anisotropy in silicon nitride with aligned reinforcing grains. *Journal of the American Ceramic Society*. 2000; 83(3):663-665.
- Imamura H, Hirao K, Brito M, Toriyama M, Kanzaki S. Further improvement in mechanical properties of highly anisotropic silicon nitride ceramics. *Journal of the American Ceramic Society*. 2000; 83(3):495-500.
- Costa C, Todd J. The role of  $Si_3N_4$  whiskers on the fracture toughness and reliability of  $Si_3N_4$  ceramics. *Cerâmica*. 1997; 43(280):95-99.
- Quinn G. The fracture toughness Round Robins in Vamas: What we have learned. In: Salem J, Quinn G, Jenkins, editors. *Fracture Resistance Testing of Monolithic and Composite Brittle Materials, ASTM STP 1409*. West Conshohocken, PA: ASTM International; 2002. p. 107-126.
- Mitomo M, Uenosono S. Gas-pressure sintering of  $\beta$ -silicon nitride. *Journal of Materials Science*. 1991; 26:3940-3944.
- Tani E, Umabayashi S, Kishi K, Kobayashi K, Nishijima M. Effect of Size of Grains with Fibre-Like Structure of  $Si_3N_4$  Fracture Toughness. *Journal of Materials Science*. 1985; 4:1454-1456.
- Peillon F, Thevenot F. Microstructural designing of silicon nitride related to toughness. *Journal of the European Ceramic Society*. 2002; 22:271-278.